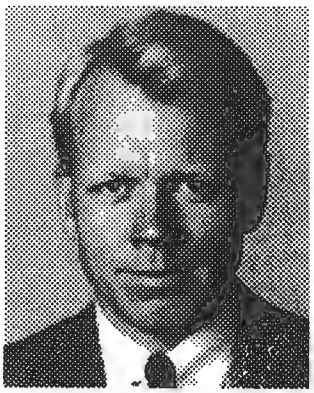

PLAIN AND STEEL FIBER REINFORCED CONCRETE BEAMS SUBJECTED TO COMBINED MECHANICAL AND THERMAL LOADING

Ali Alavizadeh-Farhang, M. Sc., Ph.D. Student
Dept. of Structural Engineering
Royal Institute of Technology (KTH)
SE-100 44 Stockholm, Sweden

Johan Silfwerbrand, Ph.D., Professor
Dept. of Structural Engineering
Royal Institute of Technology (KTH)
SE-100 44 Stockholm, Sweden

ABSTRACT

The paper describes tests on combined mechanical and thermal loading on plain and steel fibre reinforced concrete beams. The beams were subjected to solely thermal, solely mechanical and combined thermal and mechanical loads, while the rotation of the beam at supports was prevented. In order to estimate the degree of restraint, some simply supported beams were also tested and the results were compared with the results from restrained tests. Heating the top surface of the test beams provided thermal load, whereas mechanical load was introduced by applying a point load at mid-span of the test beams. The induced thermal gradient, applied mechanical load, strain distribution across the critical sections and vertical and horizontal deformations along the beam were monitored. The test results conducted on both plain and steel fibre reinforced beams showed that the superposition of stresses for combined loading gave a satisfactory estimation of the load-carrying capacity. The results also showed that the effect of relaxation of stresses due to short time thermal loads was not noticeable in the achieved load-carrying capacity for combined tests. On the contrary, a tendency for reduction of load-carrying capacity was observed at higher thermal gradients.

In addition, the ductile behavior of steel fibre reinforced concrete after cracking and release of thermal stresses due to reduction of stiffness are the most important observations in steel fibre reinforced concrete beams. Using the residual load-carrying capacity of cracked steel fibre reinforced concrete and neglecting the thermal stresses may lead to a reduction of concrete thickness in structural design.

Key words: combined loading, thermal loads, load carrying capacity, steel fibre reinforced concrete, plain concrete, beam tests

1 INTRODUCTION

Concrete structures are generally subjected to various kinds of loads with dissimilar properties. The most common group of loads may be defined as mechanical loads, static and dynamic loads, to which concrete structures are frequently exposed. In addition to mechanical loads, restraint loads are another essential category of loads, which are caused by restrained movements such as expansion, contraction and curvature of the concrete structures. Restrained loads usually occur as a result of blocked thermal movement, prevented shrinkage and unwanted support settlement. A great deal of research has been successfully conducted, studying the behavior of concrete structures subjected solely to either mechanical or restrained loads. On the contrary, only a small percentage of the efforts has been dedicated to the understanding of the real behavior of concrete structures subjected to combined loading. The results of this research aim to improve the design rules for concrete bridge decks and concrete pavements subjected to combined mechanical and thermal loads.

In both bridge deck and pavement design, it is usual to consider two types of stresses: (i) those produced by applied mechanical loads, e.g., traffic loads, and (ii) those produced by restrained loads such as thermal and shrinkage loads. These stresses are usually computed separately and the results are subsequently added. Considering the fact that most of concrete structures are exposed simultaneously to combination of loads, which may have different magnitude and duration, could lead to a more complex structural response. Consequently, the developed stresses in a concrete road or bridge deck due to combined loads may be different from the traditional computation approach. Several factors could influence the stresses:

(i) The non-linearity of thermal gradients leads to internal restraint in the concrete section. This leads to self-equilibrating stresses, which in many cases reduce the magnitude of tensile stresses and reform the stress distribution across the depth of concrete structures.

(ii) The duration of diurnal thermal gradients and subsequent thermal stresses is some hours, whereas duration of traffic load is parts of a second. The short time creep for thermal stresses is a function of stress-strength ratio, time and temperature. Relaxation of the thermal stresses may lead to increased load-carrying capacity of the structure.

(iii) The high magnitude of thermal loads may cause cracking with subsequent reduction of stiffness. This leads to a reduction of restraint moment and subsequently a lower stress level will be achieved in conventionally reinforced and steel fibre reinforced concrete structures.

These effects mean that calculation of stresses by use of superposition is likely to be an approximate method that could overestimate the acquired stresses in the concrete pavement. The aim of this project is mainly to expand the existing knowledge of the real behavior of plain and steel fibre reinforced concrete beams, due to combined mechanical and restrained loads and, finally, to improve design rules for concrete structures.

The aim of this research is to study the behavior of plain, steel fibre reinforced and conventionally reinforced concrete beams subjected to combined loading. However, the present paper deals with the test results and observations from the tests on plain and steel fibre reinforced concrete beams. The analysis of test results from conventionally reinforced concrete beams subjected to combined loading is under progress and will be published in the near future.

2 BEAM DETAILS AND TESTING PROCEDURE

The experimental plan developed for this study involved two test series including 10 and 14 beam tests, respectively. In order to examine the test set-up and practicality of the experiments, a number of pre-tests were carried out. Furthermore, the first test series was conducted on plain concrete beams subjected to combined thermal and mechanical loads, whereas, the second test series was carried out on steel fibre reinforced concrete beams subjected to same type of load combination.

Preventing the rotation of the beam at the support provided restrained load. Thermal loading induced non-linear thermal gradients, which caused curling of the beam. The non-linear thermal gradient was introduced by heating on the top surface, and the mechanical load by a hydraulic jack resulting in a point load at mid-span.

2.1 Plain concrete beams

The first test series, which comprised 10 beams, was conducted on plain concrete beams (PCB). One beam was used in order to study the induced temperature gradients along the length, width and height of the beam. Three beams were subjected solely to ultimate point load, in which one beam was not restrained and the rest of the beams were restrained. Three beams were subjected solely to ultimate thermal load, in which one was not restrained. Three beams were subjected to different combinations of point and thermal loads, in which the thermal loads were intended to be 20 %, 40 % and 60 % of the restrained ultimate thermal load, respectively.

The nominal length l, height h and width b of the beam was 3600, 300 and 150 mm, respectively. The material strength tests were conducted according to Swedish Standard [2]. The concrete had compressive strength f_{cc} between 38,6 and 42,6 MPa (tested on cubes) and a splitting tensile strength between 3,4 and 3,8 MPa. The flexural tensile strength f_{ct} varied between 4,8 and 5,2 MPa. The modulus of elasticity E was estimated to lie between 28000 and 30000 MPa.

The beams were shear reinforced over the supports in order to avoid a shear failure, see Figure 1 (a)-(c). The arrangement of flexural reinforcement is also shown in the same figure. The beam was not provided with flexural reinforcement over a distance of 900 mm at the mid-span in order to study the behavior of plain concrete. The shear reinforcement had a quality of Swedish grade Ks 40S, which had a characteristic yield stress of about 400 MPa. The flexural reinforcement was of Swedish grade Ks 60 with a characteristic yield stress of about 600 MPa.

The thermal load was applied at the upper surface of the concrete beams. By heating the upper surface of the beam, a non-linear temperature difference was developed along the beam height. The mechanical load was applied as a four point loading with the acting mechanical loads placed at the middle part of the beam with a distance of 150 mm from each other. The self-weight load was small compared to the needed ultimate mechanical load, therefore, its effect on the measured and calculated deformations and strains was neglected.

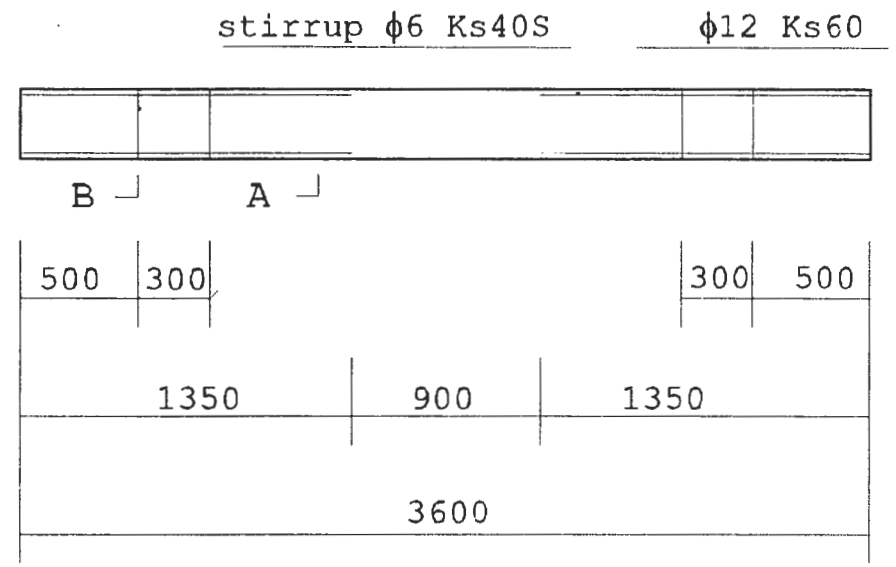

(a) Reinforcement and nominal dimensions of the test beams

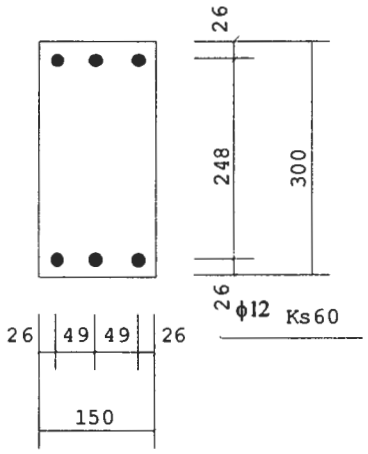

(b) Section A

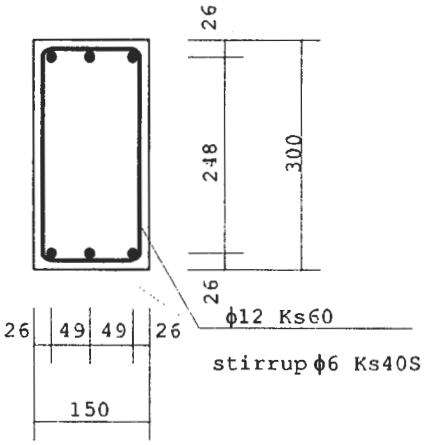

(c) Section B

Figure 1 (a)-(c) Test beam dimensions (mm) and reinforcement.

The beams were cast with ready mixed concrete, which was delivered at two different dates, therefore, the mechanical properties were slightly different.

Table 1 displays load type and support condition for the test series. Beam PCBT0 was subjected to thermal load in order to study the distribution of temperature along the length, width and height of the beam and find a proper thermal load step for the thermal testing. Beams PCBP1, PCBP2 and PCBP3 were mechanically loaded up to failure in which PCBP1 and PCBP3 were externally restrained and PCBP2 was simply supported. Beams PCBT1, PCBT2 and PCBT3 were solely exposed to thermal load in which PCBT1 and PCBT3 were externally restrained and thermally loaded to failure. Beam PCBT2 was simply supported and thermally loaded up to a certain level of temperature difference. Beams PCBPT1, PCBPT2 and PCBPT3 were subjected to different combinations of thermal and mechanical loads in which thermal load was intended to be 20 %, 40 % and 60 % of the maximum ultimate thermal load.

Table 1 Characteristics of the beams

TEST NO.	TYPE OF LOADING	SUPPORT CONDITION	LOAD ABBREVIATION
PCBT0	Thermal	Simple	ΔT_{C1}
PCBP1	Mechanical	Restraint	ΔP_{U1}
PCBP2	Mechanical	Simple	ΔP_{U2}
PCBP3	Mechanical	Restraint	ΔP_{U3}
PCBT1	Thermal	Restraint	ΔT_{U1}
PCBT2	Thermal	Simple	ΔT_{C2}
PCBT3	Thermal	Restraint	ΔT_{U2}
PCBPT1	Thermal & Mechanical	Restraint	$0.2 \times \Delta T_{U,MAX} + P_{REST1}$
PCBPT2	Thermal & Mechanical	Restraint	$0.4 \times \Delta T_{U,MAX} + P_{REST2}$
PCBPT3	Thermal & Mechanical	Restraint	$0.6 \times \Delta T_{U,MAX} + P_{REST3}$

In Table 1, ΔP_U and ΔT_U stand for the ultimate mechanical and thermal loads measured during the tests. In addition, $\Delta T_{U,MAX}$ and P_{REST} represent an approximate average value of the measured ultimate thermal loads and the rest needed mechanical load for reaching a crack failure, respectively. ΔT_C stands for a certain value of temperature difference, which was used for control tests with no failure as result.

2.2 Steel fibre reinforced concrete beams

The second test series consisted of 14 beams and concerned the behavior of steel fibre reinforced concrete under combined loads. The test specimens were named as SFRC beams and were cast with ready mixed concrete with 0,75 percent by volume of Dramix steel fibers (60 kg/m^3) with a fiber length of 30 mm and fiber diameter of 0,5 mm. The concrete was delivered in one batch, therefore, the mechanical properties should be almost constant for all beams. The steel fibre reinforced concrete had almost the same material strength as used plain concrete. For a better distribution of steel fibers, the maximum aggregate size was chosen to be 12 mm in the matrix, whereas in plain concrete the maximum aggregate size was 18 mm. The reduction of maximum aggregate size also contributed to some decrease of the variation in tensile strength.

In this group, one beam was fully instrumented with thermocouples in order to verify the induced temperature gradients along the length, width and height of the beam. Four beams were subjected to mechanical loads in which two beams were externally restrained and two simply supported. Three externally restrained beams and one simply supported were exposed to thermal loading. Six externally restrained beams were subjected to combined thermal and mechanical loads with various load ratio combinations.

All the beams had dimensions of 3600×250×150 mm. The beam height was reduced from 300 mm in plain concrete test series to 250 mm in steel fibre reinforced concrete beams in order to reduce the moment of inertia I, and by doing that, increase the degree of restraint. As for plain concrete tests, the compressive strength of the concrete f_{cc} was measured on standard cubes and

had values between 54 and 59 MPa, whereas, the tensile splitting strength f_{csp}, was obtained by cube tests, had values between 4,0 and 4,2 MPa. The flexural first-crack strength f_{flcr} and flexural ultimate strength f_{flu} were equal and varied from 4,5 to 5,1 MPa. The residual tensile strength $f_{flcr}^{(10, 30)}$ was calculated to 3,0 MPa. The flexural tensile tests on standard beams were conducted according to standard test procedures designed for steel fibre reinforced flexural beams according to [3], [4] and [5]. The modulus of elasticity E was approximated to a value between 30000 and 32000 MPa. Beside the flexural tensile test, the rest of material strength tests were conducted according to Swedish Standard [2].

The arrangement and quality of flexural and shear reinforcement is identical to the plain concrete beams. Figure 2 shows the arrangement of shear reinforcement and other beam details.

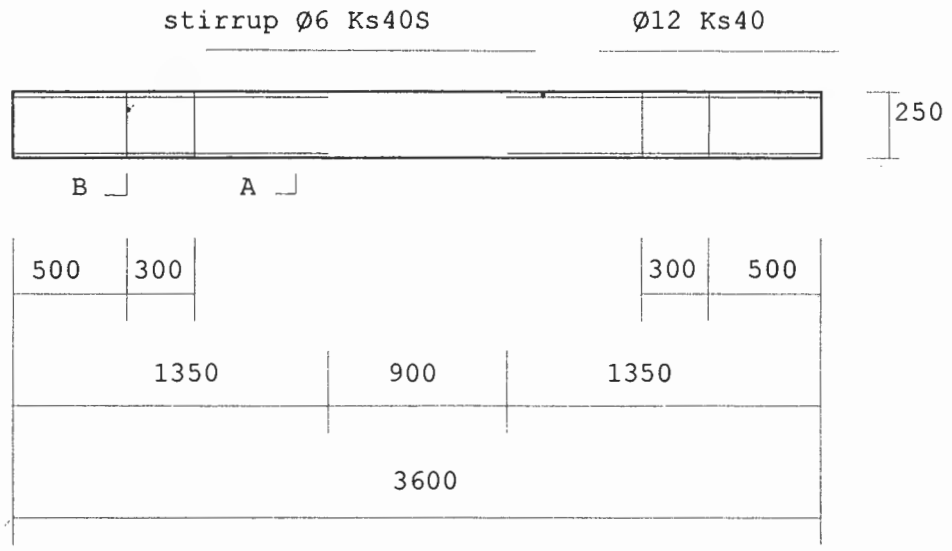

(a) Reinforcement and nominal dimensions of the test beams

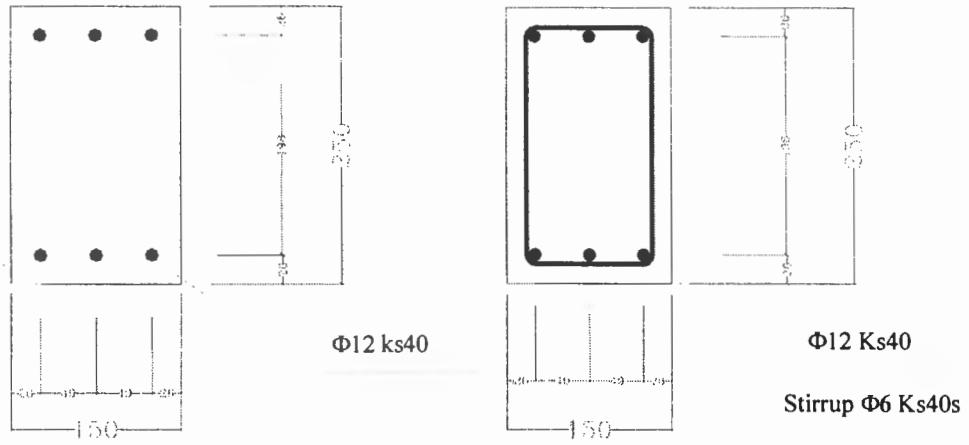

(b) Section A

(c) Section B

Figure 2 (a)-(c) Test beam dimensions and reinforcement (measurements in mm).

Table 2 displays load type and support condition for the test series. Beam SFRCT0 was used to determine if the steel fibre reinforcement could influence the thermal gradients and to find a proper thermal load step for SFRC beams. Beams SFRCP1, SFRCP2, SFRCP3 and SFRCP4 were mechanically loaded in which SFRCP1 and SFRCP3 were simply supported and SFRCP2 and SFRCP4 were externally restrained at supports. Beams SFRCT1, SFRCT2, SFRCT3 and SFRCT4 were exposed to thermal load in which SFRCT1, SFRCT2 and SFRCT3 were restrained and thermally loaded to failure whereas SFRCT4 was simply supported and thermally loaded up to a certain thermal load level that did not cause any risk for thermal cracking of the beam. Six beams SFRCPT1-6 were subjected to different combinations of thermal and point load in which the maximum achieved thermal load at failure was intended to increase gradually at each new combined loading test. In the steel fiber reinforced test series the thermal and mechanical loads were applied as the same way as in the plain concrete test series.

Table 2 Characteristics of the steel fibre reinforced beams

TEST NO.	TYPE OF LOADING	SUPPORT CONDITION	LOAD ABBREVIATION
SFRCP1	Mechanical	Simple	ΔP_{U1}
SFRCP2	Mechanical	Restraint	ΔP_{U2}
SFRCP3	Mechanical	Simple	ΔP_{U3}
SFRCP4	Mechanical	Restraint	ΔP_{U3}
SFRCT1	Thermal	Restraint	ΔT_{U1}
SFRCT2	Thermal	Restraint	ΔT_{U2}
SFRCT3	Thermal	Restraint	ΔT_{U3}
SFRCT4	Thermal	Simple	ΔT_{C4}
SFRCPT1	Thermal & MECHANICAL	Restraint	$0.2 \times \Delta T_{U,MAX} + P_{REST1}$
SFRCPT2	Thermal & MECHANICAL	Restraint	$0.25 \times \Delta T_{U,MAX} + P_{REST2}$
SFRCPT3	Thermal & MECHANICAL	Restraint	$0.3 \times \Delta T_{U,MAX} + P_{REST3}$
SFRCPT4	Thermal & MECHANICAL	Restraint	$0.4 \times \Delta T_{U,MAX} + P_{REST4}$
SFRCPT5	Thermal & MECHANICAL	Restraint	$0.6 \times \Delta T_{U,MAX} + P_{REST5}$
SFRCPT6	Thermal & MECHANICAL	Restraint	$0.7 \times \Delta T_{U,MAX} + P_{REST6}$

The $\Delta T_{u,max}$ is an average value for $\Delta T_{u,1}$, $\Delta T_{u,2}$ and $\Delta T_{u,3}$.

3 EXPERIMENTAL SET-UP

In order to study the behavior of concrete beams due to simultaneous loading, a special experiment set-up was developed. The experimental set-up introduced restraint moments at the supports as a result of restrained curling of the test beams due to induced temperature differences. The restraint of the test beam at each support was provided by use of steel rods, which were placed two by two at each side of the beam and were anchored to a counter beam. Roller supports were placed between test and counter beam in order to avoid axial forces.
Figure 3 and Figure 4 show the designed test set-up.

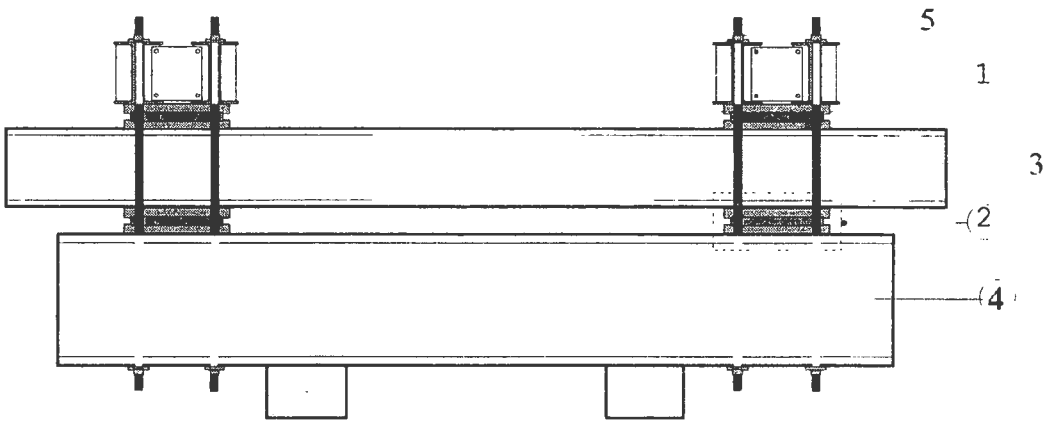

(1) Spreader beam, (2) Roller support, (3) Test beam, (4) Counter beam, (5) Tie rod

Figure 3 Longitudinal section of experimental set-up

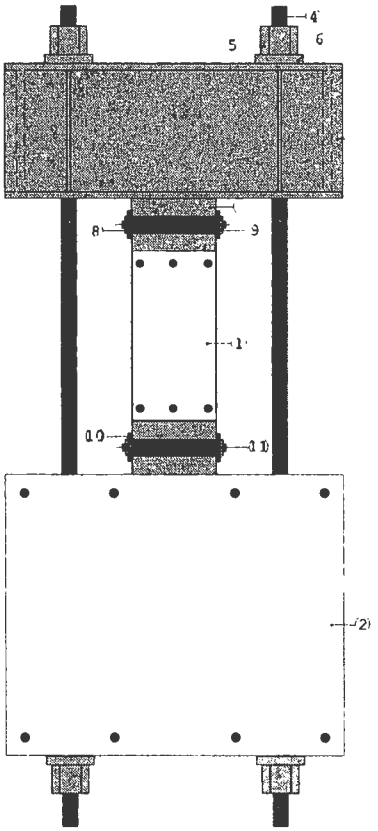

(1) Test beam, (2) Counter beam, (3) Spreader beam, (4) Tie rod, (5) Nut, (6) Steel washer, (7) Steel plate, (8) Roller support, (9) Distance holder, (10) Steel frame, (11) Screw

Figure 4 Cross section of experimental set-up.

4 INSTRUMENTATION

Concrete strains were measured with temperature compensated electrical resistance strain gauges glued to the concrete surface in four sections (A, B, C and D) in both test series, see Figure 5. The strain gauges had a length of 30 mm and width of 6 mm. The strain gauges used for the plain concrete beams were temperature compensated in a temperature range extended from -20 °C to +80 °C, whereas the strain gauges used for steel fibre reinforced beams were temperature compensated in a temperature range from –80 °C to +200 °C. For further information on the location of the gauges see Reference [1].

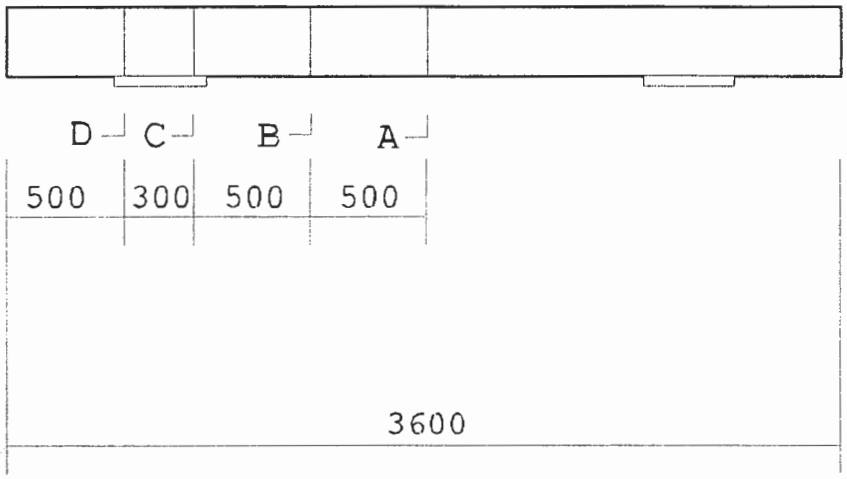

Figure 5 The position of the instrumented sections along the length of the beam (measurements in mm).

The temperature was recorded through the depth of each beam at four sections A, B, C and D by means of thermocouples cast into the plain and steel fibre reinforced concrete beams. In the plain and steel fibre reinforced concrete beams, which were subjected to thermal load or to combinations of mechanical and thermal loads, the numbers of thermocouples were about 10 and 13, respectively. For further information on the location of the thermocouples see Reference [1].

In both test series, the deflections of the beams were measured with linear variable displacement transducers (LVDTs). The vertical displacement of the plain concrete beams was measured with five LVDTs, which were placed at mid-point, quarter points and two points as close as possible to the supports see Figure 6, whereas the vertical displacement of the steel fibre reinforced beams was measured with eight LVDTs, two of them were placed at the mid-point, two of them at two quarter points, two LVDTs at two points close to the interior supports and two LVDTs at two mid-points between interior and exterior rollers, see Figure 7.

The axial expansion or contraction, caused by thermal loading, was also measured by use of two LVDTs, which were placed above the supports, at a level of half height, as it is shown in Figure 6 and Figure 7. Five of the vertically placed LVDTs had a maximum measuring capacity of 2 mm and three of them up to 20 mm, whereas the horizontally placed LVDTs had a maximum measuring capacity of 20 mm.

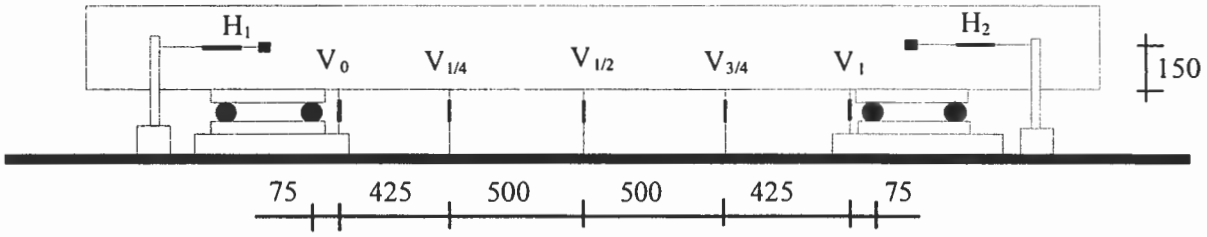

Figure 6 The position of displacement transducers placed between plain concrete test beam and counter beams (measurements in mm).

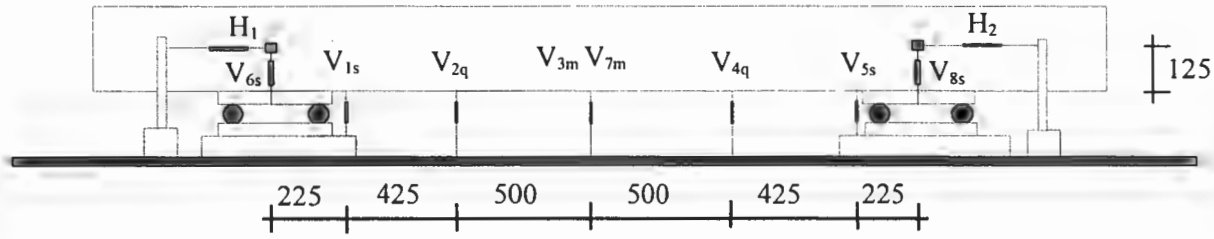

Figure 7 The position of displacement transducers placed between steel fibre reinforced concrete test beam and counter beams (measurements in mm).

The mechanical load was measured by a load cell with a maximum measuring capacity of 50 kN. In plain concrete tests, the induced forces in the tie rods were measured with strain gauges attached to the steel bars, whereas in steel fibre reinforced tests series, the induced forces in the tie rods were measured with load cells with a maximum measuring capacity of 50 kN. The thermal loading was applied by heating lamps located on the upper surface of concrete between the supports.

5 TEST RESULT AND DISCUSSION

The analysis of the test result consists of overall comparisons between measured deflection, concrete strain and ultimate loads of different combined load tests [1]. In addition, a comparison of strain distributions based on linear and non-linear temperature differences is shown here. Finally, the load carrying capacities were compared to load carrying capacities that can be obtained from superposition principle. Analysis of the test result points to several important observations, which will be discussed below.

5.1 Plain concrete beams

The thermally loaded beam PCBT0 showed that thermal heating on the upper side of the beam induced a non-linear thermal gradient in the vertical direction whereas no significant thermal gradients are observed in the longitudinal and lateral directions.

The mechanically loaded tests show a great variation in load-carrying capacity. This is because of a wide variation of flexural bending strength of the plain concrete. However, the same variation was observed in thermally loaded tests with a lower ultimate tensile strain.

Figure 8 shows load-deflection curves for externally restrained and simply supported beams (PCBP1-3). The same slopes in load-deflection curves were observed for externally restrained tests, whereas the failure appeared at various tensile strains. The very same reason causes a great variation in thermal load-carrying capacity. Figure 9 illustrates the load-deflection curves for externally restrained and simply supported beams (PCBT1-3). As for the mechanically loaded beams, the failure appeared at different tensile strain. Nevertheless, the uniform slopes of the load-deflection curves indicate that the loading procedure and support conditions were identical for externally restrained tests.

In Figure 8 and Figure 9, curves P2 and T2 with lower slopes represent load-deflection curves for simply supported beams, whereas, P1, P3 and T1, T3 represent load deflection curves for externally restrained tests under mechanical and thermal loads, respectively. One important observation is that the magnitude of maximum reached tensile strain is essentially lower in the thermally loaded beams than in the mechanically loaded beams. The measured crack stresses for the mechanically loaded test beams are almost equal to flexural tensile strength derived from the standard tests. However, an overall reduction of the flexural tensile strength is observed due to thermal loading. There are at least two factors that may affect the flexural tensile strength of plain concrete in the thermally loaded tests. One factor may be the reduction of tensile strength of plain concrete due to increase of temperature and another may be the influence of shape of stress distribution on the tensile strength at the failure section.

In both mechanically and thermally loaded tests, the failure occurred as a result of flexural bending at the mid-span of the beams, where the maximum moment due to either mechanical or thermal loads occurred. The failure appeared in form of one through crack that divides the test beam into parts.

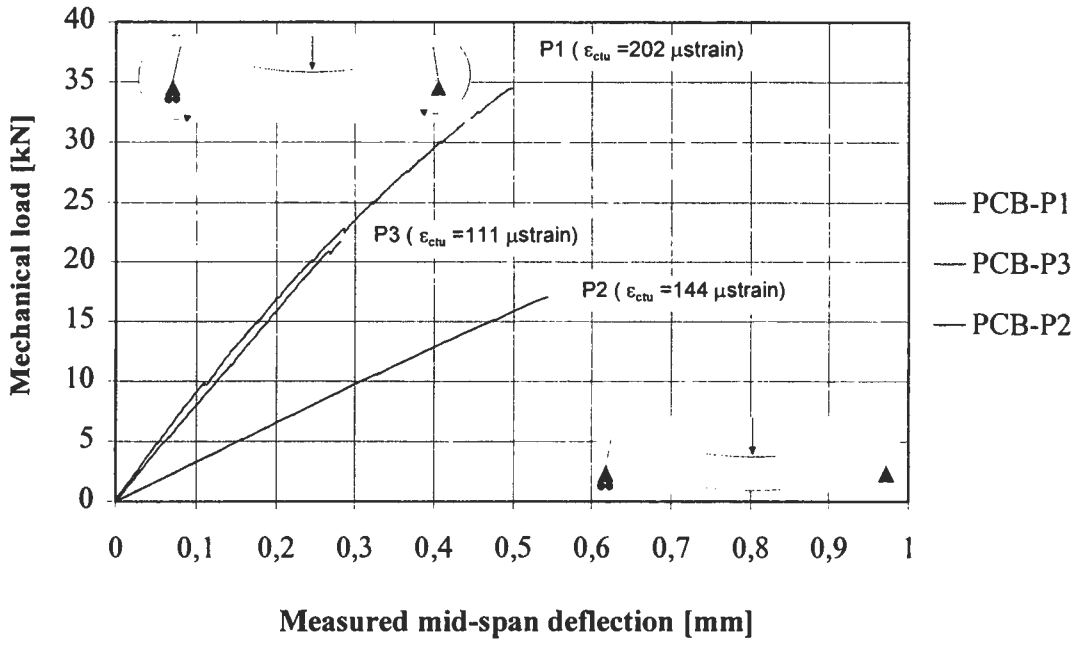

Figure 8 Load-deflection curves for mechanically loaded plain concrete beams ($\varepsilon_{ctu,max}$ is maximum measured ultimate tensile strain near the bottom edge in the mid-section).

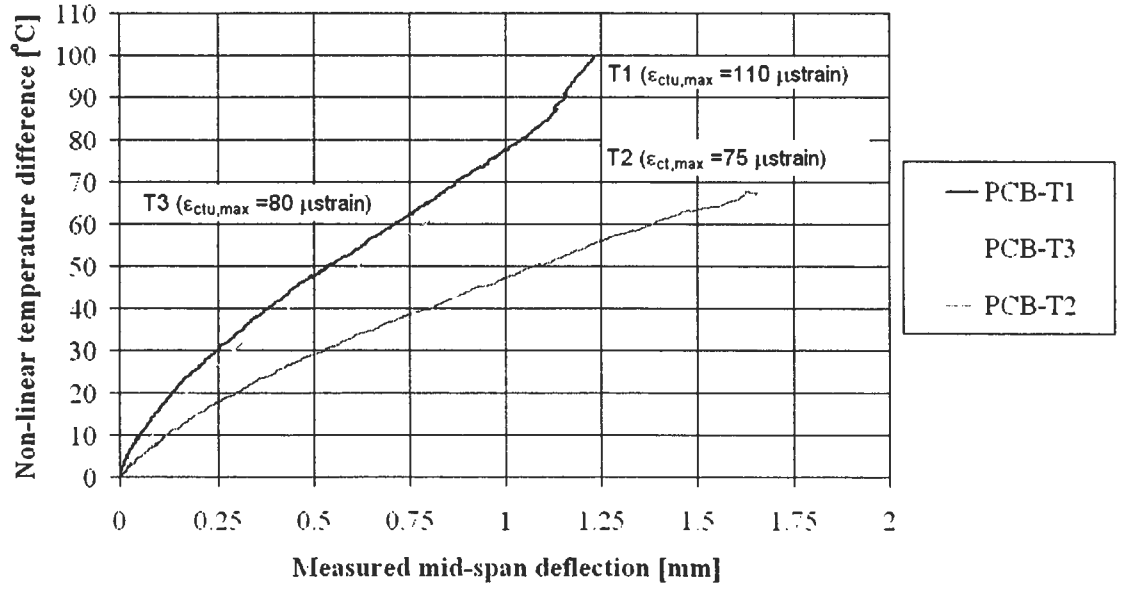

Figure 9 Load-deflection curves for thermally loaded plain concrete beams ($\varepsilon_{ctu,max}$ is maximum measured ultimate tensile strain somewhere at the mid-height of the mid-section).

The stress distribution varies due to different type of loading. Concerning thermal loads, also the distribution of temperature difference across the section affects the stress distribution. In the tests, the induced thermal gradient is non-linear. The non-linearity of the thermal gradient leads

to self-equilibrating stresses, which reduce the magnitude of the maximum tensile stress across the beam height. The magnitude of the maximum tensile stress is essential to the fatigue behavior of concrete pavements, therefore, assumption of non-linear thermal gradient has a positive impact on the mechanical load carrying capacity (fatigue criteria) of concrete pavements subjected to repeated traffic and thermal loads.

Figure 10 illustrates the presence of self-equilibrating strain across a simply supported beam due to a non-linear temperature difference of 65,5 °C. The non-linearity of the thermal gradient causes an internal restraint which leads to compressive stresses near the edges and tensile stresses in the middle part of the beam. As a result of the self-equilibrating stresses, the magnitude of the induced tensile stresses due to external forces near the bottom edge decreases, whereas, the magnitude of compressive strain near the top surface increases. The magnitude of reduced tensile stresses depends on the degree of restraint.

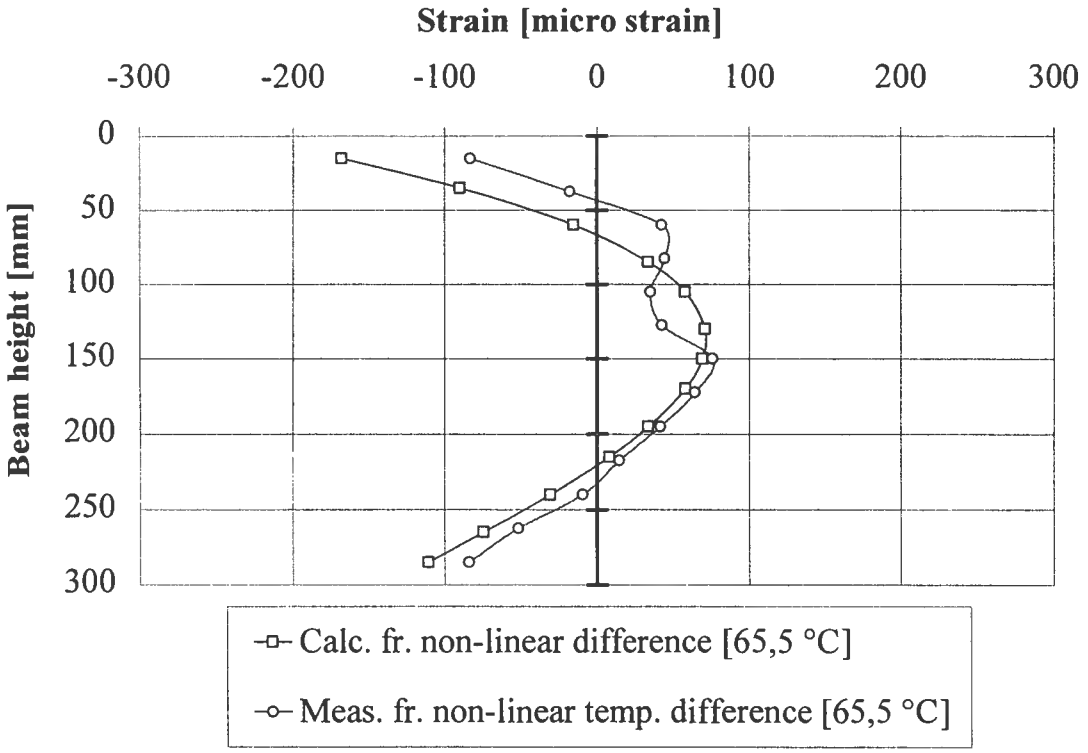

Figure 10 Self-equilibrating strain distribution (temperature compensated) in a simply supported plain concrete beam.

The experimental set-up represents a statically indeterminate structure subjected to mechanical load at the mid-span and equally distributed thermal heating on the top surface of the test beam. The tie rods function as springs which resisting against rotation of the beam at supports. A simple model of the experimental set-up is a beam restrained by exterior and interior springs (tie rods) at the supports. The model provides 55 % and 75 % of the degree of restraint in a fully restrained plain and steel fiber reinforced test beam, respectively. Knowing the degree of restraint, the strain distribution across the most critical section, mid-section, can be calculated. In addition, a simple modeling of the restraint supports, as an elastic spring system that partially constrains the rotation of the beam at the supports, leads to the very same degree of restraint, see chapter 4 in [1]. Figure 11 shows measured and calculated strain distributions for test beam PCBT3 at ultimate thermal load. The linear temperature distribution with a magnitude of 67 °C

gives essentially greater tensile stress and strain than the non-linear temperature distribution. However, the measured and calculated strain distributions based on a non-linear temperature distribution are almost identical in form and magnitude. This shows that by knowing the distribution of the induced thermal gradient and the present degree of restraint, it is possible to determine the real stress distribution across the cross-section of any concrete structure. As it can be seen, the magnitude of maximum tensile strain caused by a linear thermal gradient is almost twice the corresponding value due to a non-linear thermal gradient. As it is known, the stress magnitude difference affects the mechanical load-carrying capacity of concrete structures subjected to repeated combined loading ([6] and [7]).

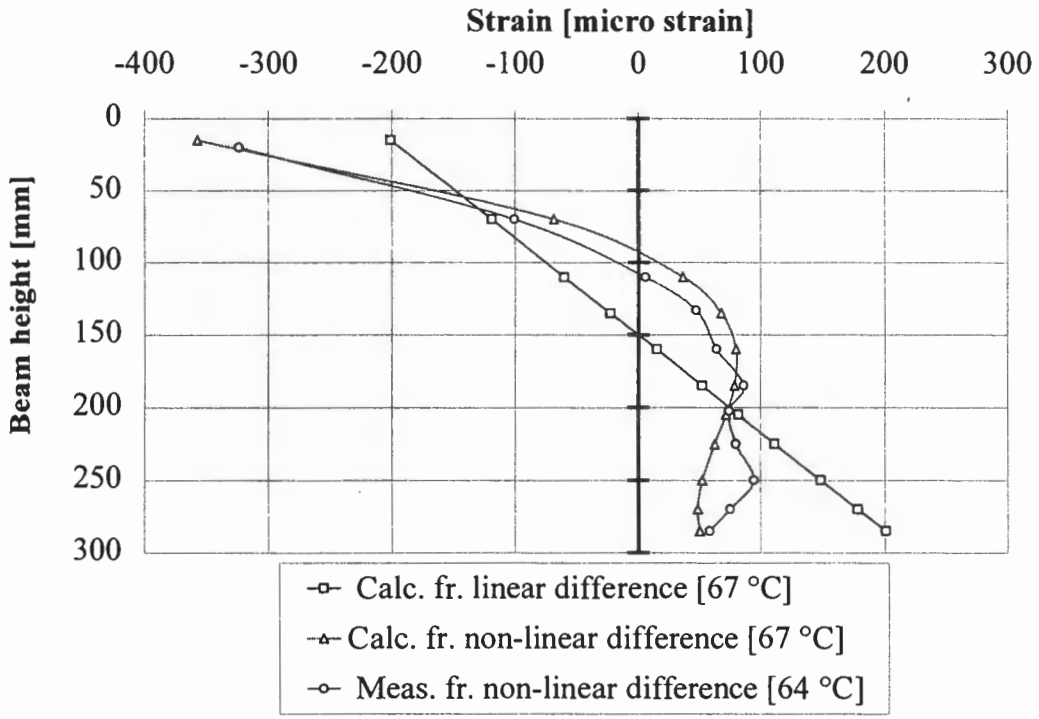

Figure 11 Strain distribution across the beam PCBT3.

Table 3 shows the ultimate load of solely mechanical, solely thermal and combined mechanical and thermal tests on plain concrete beams.

Table 3 Observed ultimate loads for plain concrete beams.

Test	Support condition	Mechanical load [kN]	Temperature difference [°C]
PCBP1	Restraint	34,5	-
PCBP2	Simple	17	-
PCBP3	Restraint	21,5	-
PCBT1	Restraint	-	100
PCBT2[1]	simple	-	65
PCBT3	Restraint	-	67
PCBPT1	Restraint	25,5	27,5
PCBPT2	Restraint	18,0	42,5
PCBPT3	Restraint	11,3	57,5

[1] *No failure was observed*

There were no load-carrying capacity left after cracking of the concrete. The single failure crack was initiated from the tensile side and passed through the whole cross section.

The variation of mechanical load-carrying capacities for combined loading is illustrated in Figure 12.

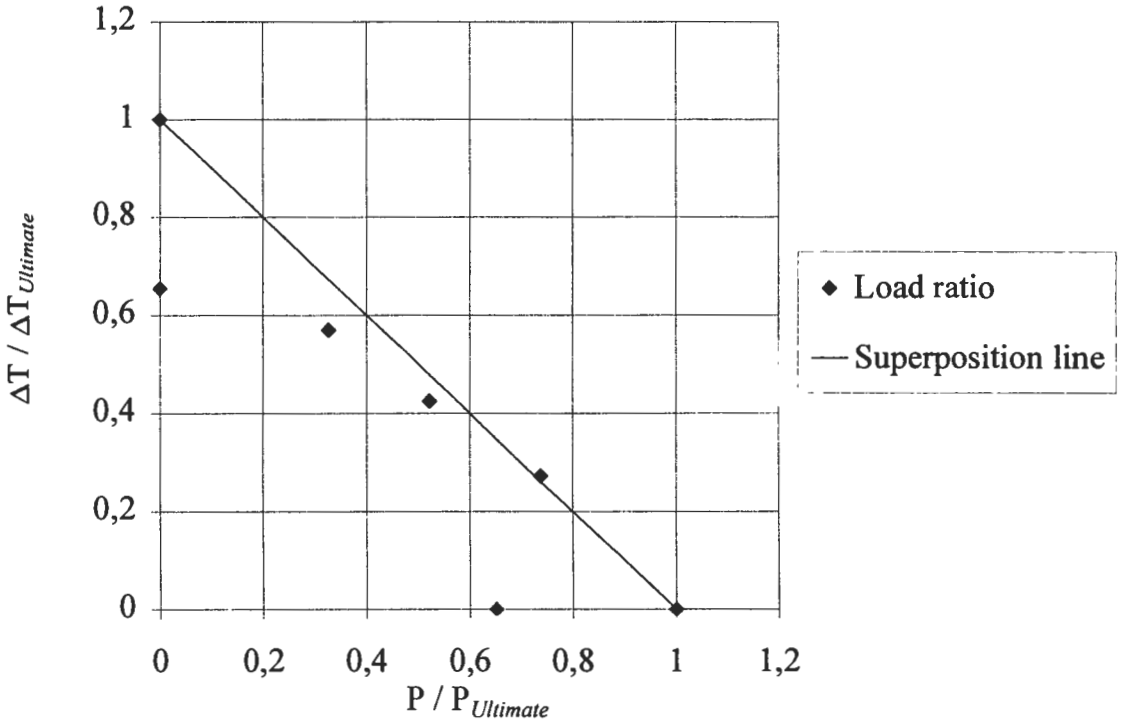

Figure 12 Interaction of combined loading for plain concrete beams (tests with higher thermal and mechanical loads were taken as ultimate loads because the measured tensile strain in the tests were closer to ultimate strain obtained by standard material tests)

The measured ultimate loads due to combined loading are grouped around the superposition line and show that superposition of loads can be a fairly good estimate for load-carrying capacity in combined loading. However, a tendency was observed regarding high thermal loads. The tensile strength and, consequently, the load carrying capacity are reduced when the beam is exposed to combination of higher thermal gradient and lower mechanical load.

The standard material strength tests conducted on flexural bending beams and splitting cubes indicate that in mechanical loading tests, the flexural tensile strength is a better representative for tensile strength, whereas in thermally loaded beams the splitting tensile strength is a more accurate value for tensile strength of the beam. The ultimate thermal and mechanical loads are assumed to 100 °C and 34,5 kN respectively, with a maximum ultimate strain value of 110 μ strain for thermal and 200 μ strain for mechanical tests.

In the three combined loading tests PCBPT1-3, the maximum thermal loads were 27 %, 42,5 % and 57 %, respectively, of the ultimate thermal load, whereas the maximum mechanical loads were 75 %, 52 % and 32 %, respectively, of the ultimate mechanical load. The sum of load

ratios in respective tests is 102 %, 94,5 % and 89 %, respectively. This indicates a decrease of load-carrying capacity due to increased thermal gradient.

The previous interaction diagram between load ratios could be expressed in another manner. Based on the measured ultimate mechanical and thermal loads and the measured flexural tensile strength, the stress-strength ratios for solely mechanical, solely thermal and combinations of mechanical and thermal loads were calculated. The derived formulas for beam model on spring supports, see chapter 4 in [1], were used to calculate the mechanical and thermal stresses. Then the stress-strength ratios were shown in Figure 13. As can be seen in the interaction diagram, the deviation of stress-strength ratios from the superposition line increases with increased share of thermal stresses. In Figure 13, the stress-strength ratios are grouped around the linear trend line as the same manners as the load ratios are grouped around the superposition line, compare to Figure 12.

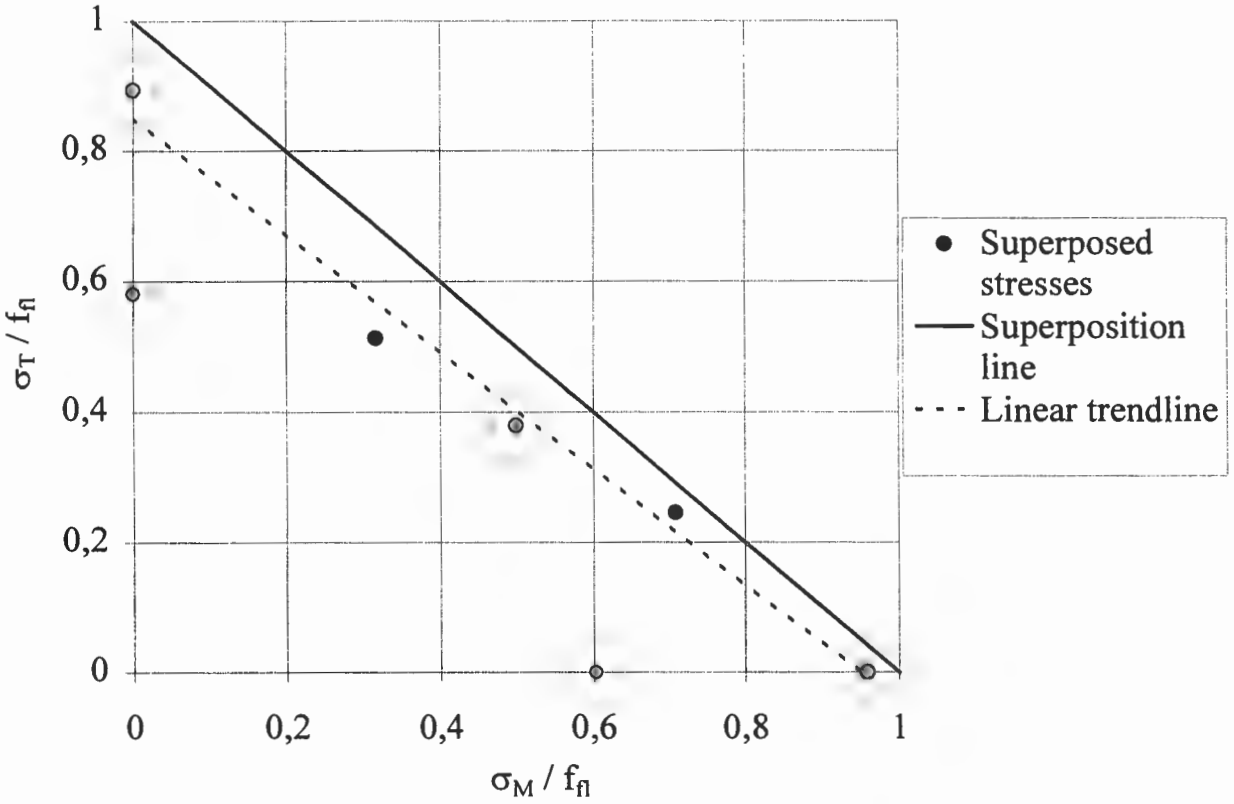

Figure 13 Interaction of stress-strength ratios (plain concrete test series)

There are possibly two reasons for a reduction of load carrying capacity due to combined loading. One reason could be a possible reduction of the flexural tensile strength of concrete due to higher concrete temperature. It is known that increase of concrete temperature could decrease the compressive strength of concrete by 20 percent [8]. However, the effect of short time thermal loading on flexural tensile strength is not given in [8]. An investigation on the influence of temperature and stress level in bended concrete beams on concrete properties such as short time creep, relaxation and flexural tensile strength is progressing by the authors at the Royal Institute of Technology (KTH) in Sweden.

Concrete contains numerous microcracks caused by applied loading or already existing before loading. The process of development and unification of microcracks governs the reduction of stiffness and the magnitude of achieved ultimate tensile strength of a concrete beam.

Another possible reason could be a reduction of tensile strength due to developed or widening of already existing microcracks inside the concrete due to thermal loading. The damage process or microcracking of concrete depends strongly on the applied lateral stress, the magnitude of tensile stress and the largeness of exposed area under the tensile stress. The variation of observed ultimate tensile strain between mechanically and thermally loaded beams may be dependent on the way microcracks develop and contribute to damage process. In higher levels of thermal gradients, the tensile area is subjected to a relatively high constant tensile stress, which may lead to a more pure tensile failure. The probability of failure under constant tensile stress across the tensile area increases due to presence or development of microcracks in the tensile area. Contrary, in flexural bending the highest stress appears at the bottom edge and the presence of microcracks inside the concrete is not as essential as for a pure tensile failure.

The two above-mentioned explanations can explain why the ultimate measured strain in the thermally loaded tests are less that measured ultimate strain at the mechanically loaded tests.

Furthermore, it is noticeable that the variation of load-carrying capacity due to variation of tensile strength between the limited number of test beams does not allow a positive detection of any increase or decrease of load-carrying capacity of the beam due to other involved parameters in combined loading tests.

5.2 Steel fiber reinforced beams

As it was mentioned in subsection 2.2, the degree of restraint was increased by increasing the diameter of restraining tie rods and decreasing the beam height from 300 mm to 250 mm. A higher degree of restraint (75 %) was achieved, and consequently a more realistic ultimate temperature differences were obtained.

The behavior of steel fiber reinforced concrete before reaching the crack load is almost the same as for plain concrete. Therefore, a more brief report on ultimate loads is considered to be of interest here.

After thermal loading of SFRCT0 it was clear that the presence of steel fibers did not affect the temperature distribution in any direction and the only vital thermal gradient existed in the vertical direction.

The mechanically loaded beams, SFRCP1-4, point to the fact that the measured strain at the bottom edge in the standard flexural beams rapidly increases when the magnitude of tensile strain at the bottom edge becomes higher than 125 μ strain. This strain value is locally lower than the maximum strain given by the material tensile strength. However, the rupture of material and reduction of stiffness can be reached at higher loads. In plain concrete beams, cracking leads to a rapid rupture of the beam. In steel fiber reinforced beams, the load carrying capacity may increase even after the beginning of the crack propagation. The process of crack unification and propagation is a ductile process due to presence of steel fibers embedded in the matrix. In addition, the modulus of rupture f_{flu} is higher than the pure tensile strength f_{flcr} of the material. The observed measured strains from the mechanical tests indicate that the tensile strain related

to the tensile strength of concrete is between 100 and 120 μ strain. After this strain level, the tensile strain at the bottom edge rapidly increases, see Figure 14.

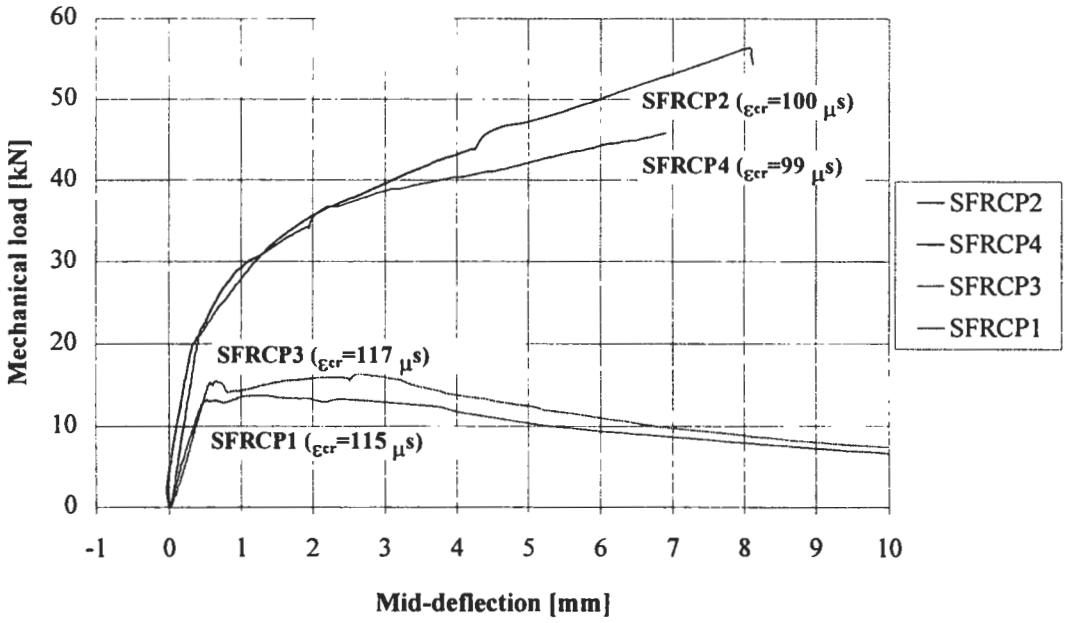

Figure 14 Load-deformation curves measured at mid-span for simply supported test beams SFRCP1,3 and for externally restrained test beams SFRCP2,4

For the simply supported beams, it was observed that the load-carrying capacity slightly increases after cracking and reaches an ultimate load higher than the crack load. The steel fiber reinforced concrete turns out to be slightly strain hardening. The load carrying capacity decreases gradually after reaching the ultimate load with increasing deformation. The cracked section functions as a plastic hinge where all the plastic rotation of the SFRC beam takes place. However, the load carrying capacity of the externally restraint beams, SFRCP2 and SFRCP4, after the cracking came as a result of the moments introduced by the external supports. They resisted the rotation of the beam at the supports. The observed failure occurred in a ductile manner. A clear flexural bending failure occurred for all mechanically loaded beams.

Steel fibre reinforced concrete is a highly heterogeneous material consisting of cement paste, aggregates, fibers, voids and microcracks. When concrete is subjected to tensile loading, micro cracks develop locally at the weakest points. During further loading these microcracks join and the overall deformation localizes into a zone at the weakest section and, subsequently, a fracture zone develops. After reaching the crack load, a macroscopic crack across the beam appears and the steel fibers begin to act solely and transfer tensile forces through the cracked section. The reduction of load carrying capacity is usually due to pullout failure of fibers. The regions outside the crack zone will unload and the stress will decrease. However, the deformation along the beam is increasing during the unloading phase. The concrete failure may be defined as the stage in which the deformation and stiffness of the beam reach critical values.

The thermally loaded beams show that the self-equilibrating stresses effect the stress distribution in the same way as stress distribution in plain concrete beams. In addition, an overall reduction of measured ultimate strain was observed in comparison to corresponding values in mechanically loaded beams. In addition, thermally loaded beams show that even after cracking

there is still a great load carrying capacity left. Figure 15 illustrates the measured deflections along the length of beam SFRCT1 at various temperature differences. The highest curve in Figure 15 represents the ultimate deflections before failure at the ultimate temperature differences.

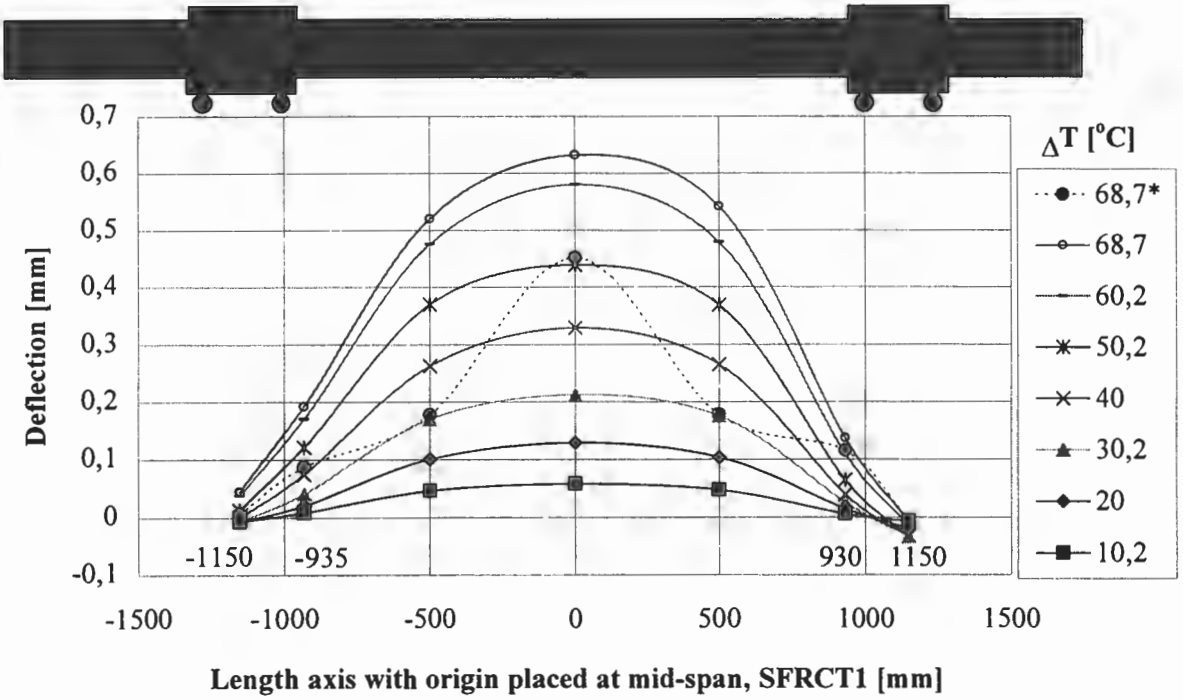

Figure 15 Beam deflection at various temperature differences for restrained test beam SFRCT1 (stands for thermal deflection of the beam after cracking)*

After cracking, a reduction of stiffness results in relaxation of thermal stresses. The end-moments at both supports were dramatically reduced. However, the most important aspect of using steel fibre reinforced concrete in concrete structures is the ability of bearing load after cracking. The crack development stopped at a distance of $0{,}2 \cdot h$ from the top edge, where h is the beam height. Mechanically loaded tests on simply supported cracked beams show that approximately 50 - 100 % of load carrying capacities were left in the cracked beams. A reduction of stiffness and ability to transfer stresses due to action of fibers make the cracked section work like a plastic hinge. This leads to less restraint moment because of the thermal load, but at the same time larger deformation under the beam because of the mechanical load. Using the large mechanical load-carrying capacity (fatigue capacity) after cracking in a cracked steel fibre reinforced concrete pavement, which does not develop large restraint loads, together with a stiff subbase may be a way to decrease the thickness of concrete pavements. The fact that the crack cannot reach the concrete surface as long as surface concrete is in compression protects the concrete from the most common environmental deterioration processes. Table 4 illustrates the ultimate mechanical and thermal loads for SFRC beams.

In Table 4, the achieved mechanical and thermal loads are given for SFRC tests. In addition, the residual loads for cracked beams and the corresponding deflection are given. In the residual load carrying capacity tests, the beams were originally cracked either due to solely thermal loading or combined loading with high share of thermal loads. The cracked beams were simply supported and subjected to mechanical load. As can be seen, the deflection values vary from 0,67 to 2,5

mm, whereas in uncracked simply supported tests the maximum deflection at crack load was measured between 0,5 and 0,7 mm. The deflections of the cracked beams were 3-4 times greater than the deflections of uncracked beams.

Table 4 Observed ultimate and residual loads for steel fibre reinforced concrete beams.

Test beams & Support conditions[1]	Mechanical load [kN] & Crack deflection [mm]	Thermal load [°C]	Residual load [kN] [2] & Maximum deflection [mm]
SFRCP1s	13,1 (0,50)	-	-
SFRCP2r	21,8	-	-
SFRCP3s	15,3 (0,70)	-	-
SFRCP4r	20,3	-	-
SFRCT1r	-	70	14,2 (0,67)
SFRCT2r	-	53	13,9 (1,1)
SFRCT3r	-	60	7,5 (1,7)
SFRCT4s[3]	-	70	-
SFRCPT1r	10,7	25,3	13,2 (1,25)
SFRCPT2r	7,7	36	16,2 (0,94)
SFRCPT3r	2,7	40	10,7 (0,94)
SFRCPT4r	12,7	14	12,5 (2,35)
SFRCPT5r	15,8	18	9,6 (2,23)
SFRCPT6r	19,7	12,5	-

[1] *suffixes r and s stand for restrained and simple support condition*
[2] *Residual load after cracking*
[3] *No failure was observed*

Figure 16 shows the load-deflection curves for two simply supported uncracked beams (thicker lines) and eight simply supported cracked beams (thinner lines) subjected to mechanical loading.

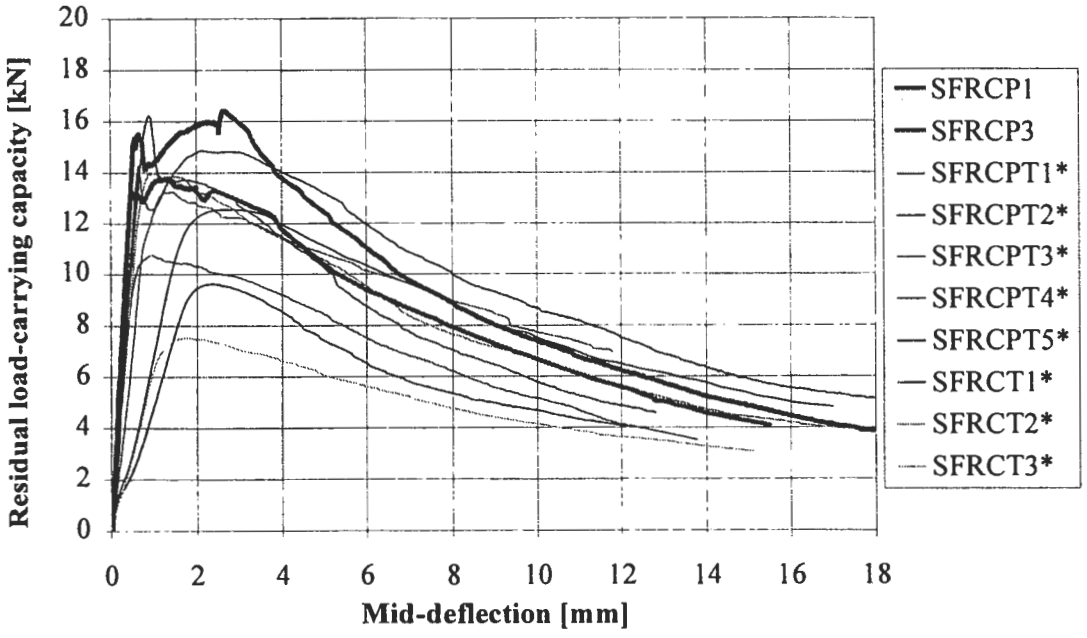

Figure 16 Load-deflection curves for the simply supported cracked and uncracked beams

Figure 17 shows the interaction between mechanical and thermal loads at crack load stage for steel fibre reinforced test beams.

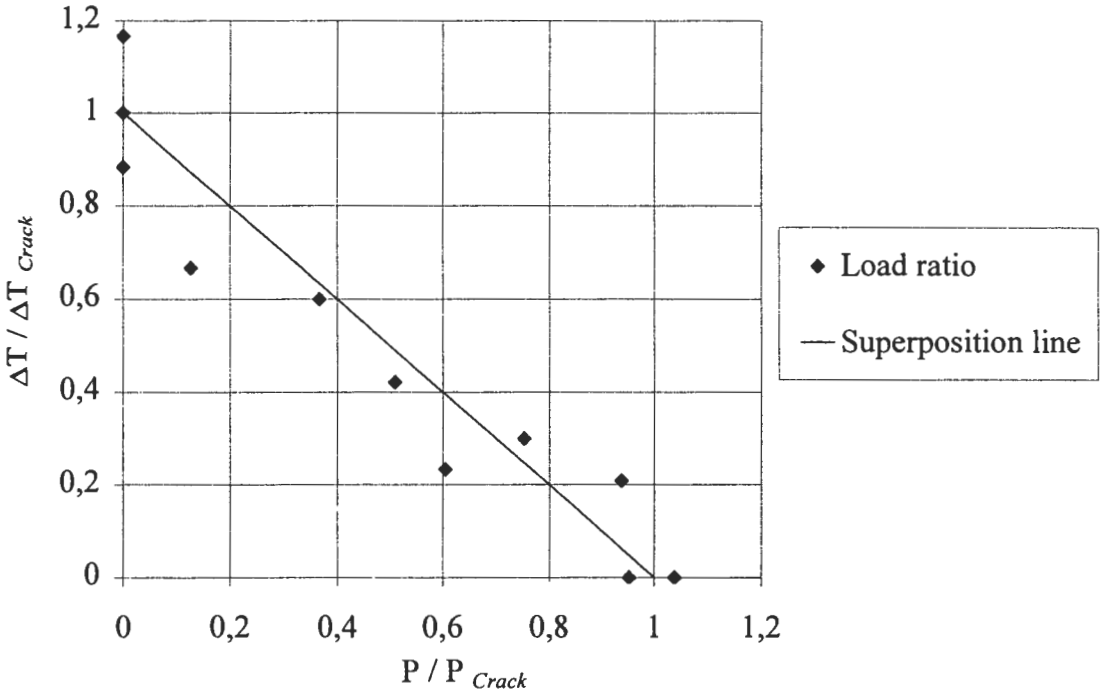

Figure 17 Interaction of load ratios at cracking stage (steel fibre reinforced concrete)

The same overall tendency as for plain concrete beam was observed in steel fibre reinforced beams. The superposition line seems to be a good approximation for estimating the load-carrying capacity up to cracking for combined loads. However, after cracking, the load carrying capacity depends on the properties of steel fibers, such as fibre content, aspect ratio, and fibre strength and fibre distribution. The variations of mechanical and thermal crack loads were less than the variation of corresponding values for the plain concrete beams. However, a 5-15 % variation of ultimate loads can be observed.

Figure 18 shows the stress-strength ratios at cracking stage for SFRC tests. As it can be seen again, a reduction of flexural tensile strengths was observed for the tests with higher share of thermal loads. When it comes to the mechanically loaded beams, the applied cracking stresses were almost as high as the flexural tensile strength of concrete (5 MPa), whereas in thermally loaded beams the applied cracking stress induced by thermal loads were lower than the flexural tensile strength of concrete. In addition, the stress-strength ratios in Figure 18 are grouped around the linear trendline as the way the load ratios were grouped around the superposition line in Figure 17.

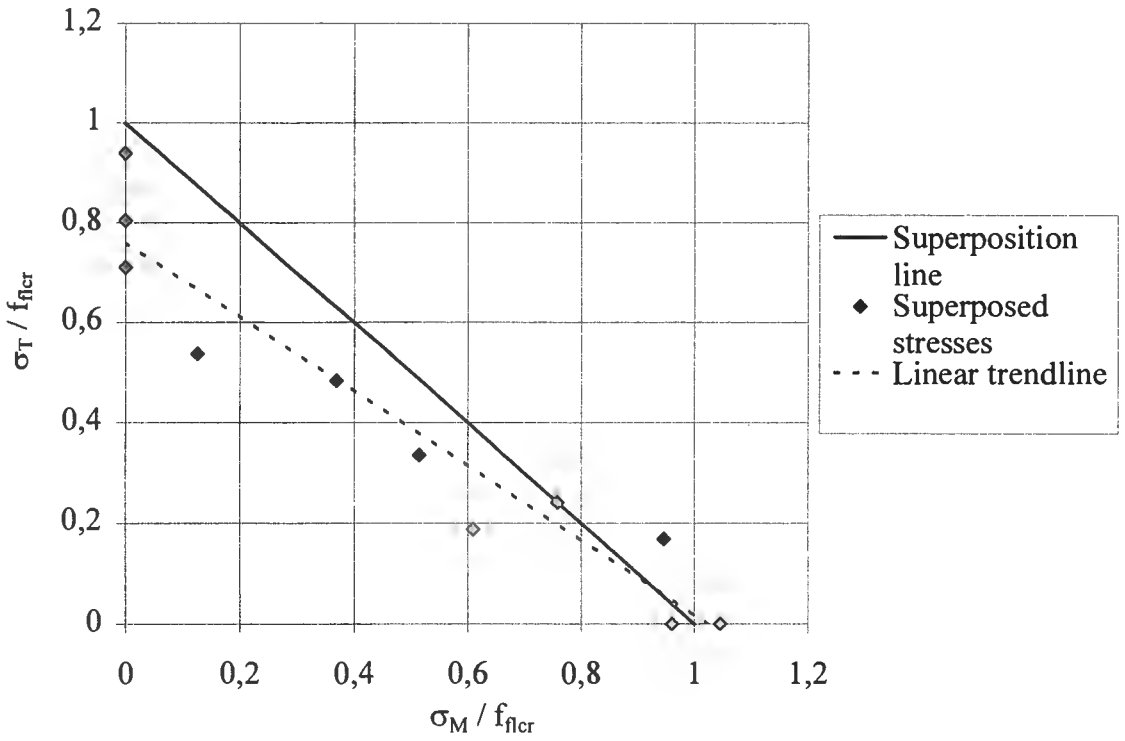

Figure 18 Interaction of stress-strength ratios at cracking stage (steel fiber reinforced concrete)

The test result also showed that the nature of thermal response of steel fibre reinforced concrete structures is such that cracking actually relieves part of the restraint forces. The typical pattern in the behavior of steel fibre reinforced structures is such that as the temperature increases, the restraint forces increase until the concrete cracks. Due to cracking and reduction of stiffness, a great part of restraint loads disappears. Then with the further increase in temperature, the restraint forces increase, but at a much slower rate than before cracking. Therefore, the maximum magnitude of these restraint forces due to very high temperature differences can approximately be equal to the magnitude of restraint forces shortly after the cracking.

It is known that a pavement must be thick enough to accommodate the flexural stress imposed by traffic and thermal loading. However, a reduction of concrete thickness will finally lead to a cracked pavement with reduced stiffness which leads to less deflection and less induced restraint moments. The very essential factor in such a design, is the sufficient mechanical load-carrying capacity after cracking. Since traffic induced stresses are repetitive, a reasonable residual stress capacity must be established to insure performance under repeated loading. In comparison with conventional concrete pavement, a steel fibre reinforced concrete pavement could be relatively flexible due to its reduced thickness and stiffness. The magnitude of anticipated elastic deflections must be assessed, because excessive elastic deflections increase the danger of pumping in subgrade beneath the slab. Stresses in the underlying layers are also increased due to reduced thickness and these must be kept low enough to prevent introduction of pavement deformation in supporting materials.

The all above-mentioned observations lead us to the conclusion that steel fibre reinforced concrete may be an attractive alternative to plain concrete pavements. In addition, the possibility of casting longer and thinner slab with fewer joints may contribute to a reduction of construction costs in order to compensate the higher material costs due to use of steel fibers in concrete.

6 CONCLUSIONS

The main conclusions from this research are the following:

1. A versatile test set-up has been developed for studying concrete beams subjected to combined mechanical and thermal loads.

2. Considering the fact that plain concrete has a wide variation of tensile strength, distinguishing the effect of temperature on load-carrying capacity of beam from the variation of tensile strength on load-carrying capacity of the beam requires a test series with a large number of specimens.

3. The non-linearity in temperature distribution creates a self-equilibrating stress in concrete. This stress in its turn leads to a reduction of the maximum tensile stress across the beam height and changes the form of stress distribution. As a result, the load-carrying capacity under fatigue loads, which is a function of stress variation (from a minimum thermal stress to a maximum sum of the traffic and thermal stresses) will be positively affected.

4. A comparison between thermally and mechanically loaded beams indicates that different tensile strength may be valid for each type of load. However, the number of the tested beams is not large enough to draw a general conclusion. Further research on the smaller beam specimens is in progress to verify if the temperature has some influence on the flexural tensile strength.

5. The result from combined loading tests does not point to an increase of load-carrying capacity due to the duration differences in loads and relaxation of the thermal stresses. On the contrary, the above mentioned observation in conclusion No. 4 may be the reason why beams with a higher share of thermal load has a greater deviation from the superposition line in both plain and steel fibre reinforced beams.

6. Considering the non-linear part of the temperature distribution that reduces the maximum tensile stress might contribute to a thinner pavement. However, a second contribution to reduction of thickness may achieve by allowing a longer steel fibre reinforced concrete slab to crack which leads to relaxation of a great part of thermal stresses. This could reduce the number of joints per unit length of the pavement. Using the residual load carrying-capacity of steel fibre reinforced concrete together with its good fatigue behavior can be a way to design more slender concrete pavements.

7 ACKNOWLEDGEMENT

The first author would like to express his sincere gratitude to the laboratory staff, who kindly helped him through the experiments. The authors would like to acknowledge *Swedish National Road Administration, The Swedish Council for Building Research* and *The Swedish Concrete Research Foundation* for the financial support of this work.

8 REFERENCES

[1] Alavizadeh-Farhang, A. (1998), *Plain and Steel Fibre Reinforced Concrete Beams Subjected to Combined Mechanical and Thermal Loading*, Licentiate thesis, Department of Structural Engineering, Royal Institute of Technology, Bulletin No. 38, Stockholm, Sweden, 1998, 298 pp.

[2] BST Byggstandardiseringen (1987). *Betongprovning med svensk standard.* BST Handbook 12, Fifth Edition, Grunditz & Forsberg Tryckeri AB, Linköping, Sweden, 1987, 272 pp. (In Swedish).

[3] ACI Committee 544 (1988). *Design Considerations for Steel Fibre Reinforced Concrete*. ACI Structural Journal, V. 85, No. 5, 1988, pp. 563-580.

[4] ASTM Standard C1018 (1992). *Standard Test Method for Flexural Toughness and First Crack Strength of Fibre Reinforced Concrete*. 1992 Annual book of ASTM Standards, Section 4 Construction, Volume 04.02 Concrete and Aggregates. Philadelphia, USA: ASTM, 1992, pp. 510-516.

[5] Swedish Concrete Association (1997). *Stålfiberbetong – Rekomendationer för konstruktion, utförande och provning*. Concrete report No 4, 2nd Edition, Stockholm, Sweden, 1997, 133 pp. (In Swedish).

[6] Palmgren A. (1924). *Die Lebensdauer von Kullagern*, Zeitschrift des Vereines deutscher Ingenieure, 1924(68):14, pp. 339-341.

[7] Miner M. A. (1945). *Cumulative Damage in Fatigue*. Journal of Applied Mechanics, Transaction of the ASME, 1945(12):1, pp. A159-A164.

[8] AB Svensk Byggtjänst och Cementa AB (1994). *Betonghandboken – material.* Second Edition, Svenskt Tryck AB, Stockholm, Sweden, 1994, 1127 pp. (In Swedish).